A New Efficient Method for Simulating Multiple Uncorrelated Rayleigh Fading Channels

Chengxiang Wang
School of EPS, EECE
Heriot-Watt University
Edinburgh Eh14 4AS, UK
cheng-xiang.wang@hw.ac.uk

Dongfeng Yuan
School of Info. Science & Engineering
Shandong University
Jinan, Shandong, 250100, P. R. China
dfyuan@sdu.edu.cn

Wen Xu
Baseband Algorithms & Standardization Lab
BenQ Mobile
Haidenauplatz 1, D-81667 Munich, Germany
wen.xu@benq.com

Abstract— **To produce multiple uncorrelated Rayleigh fading waveforms is often required for simulating wideband fading channels, multiple-input multiple-output (MIMO) channels, and diversity-combined fading channels. In this paper, a new parameter computation method for deterministic sum-of-sinusoids (SoS) channel simulators is proposed to guarantee the uncorrelatedness between different simulated Rayleigh fading processes. Numerical and simulation results show that the resulting deterministic SoS channel simulator can accurately and efficiently reproduce all the desired statistical properties of the reference model.**

I. Introduction

MIMO technologies employing multiple antennas at both the transmitter and receiver have been suggested to be used in evolved Universal Terrestrial Radio Access (E-UTRA) and Universal Terrestrial Radio Access Network (E-UTRAN) [1]. This is due to the fact that MIMO technologies can greatly improve the signal quality and enhance the system capacity. For the design and performance evaluation of such MIMO systems, a thorough understanding and an accurate modeling of the underlying MIMO channels are indispensable.

In the 3rd Generation Partnership Project (3GPP), the Spatial Channel Model (SCM) [2] and the wideband SCM [3] were recommended for simulating certain MIMO schemes, beamforming, and spatial multiplexing for bandwidths up to 5MHz and above 5MHz, respectively [4]. On the other hand, the SCM is of less interest for receiver/transmit diversity and initial space-time coding evaluations [4]. In order to simplify the initial MIMO simulation work and facilitate the rapid generation of early results for E-UTRA and E-UTRAN, there is a need to develop MIMO channel simulators which account for only temporal characteristics while neglect the spatial properties of MIMO channels. This is essentially to simulate multiple Rayleigh fading processes correlated in time but uncorrelated between processes, under the assumption of 2-D isotropic scattering environments [5]. As well as being useful for simulating MIMO channels, a channel simulator capable of generating multiple uncorrelated fading waveforms is also desirable to simulate, e.g., wideband and diversity-combined fading channels.

The sum-of-sinusoids (SoS) channel modeling approach [6], [7] has extensively been applied to the simulation of Rayleigh fading channels. In order to generate multiple uncorrelated Rayleigh fading waveforms by using SoS channel simulators, different parameter computation methods [8]–[16] have been investigated. Jakes' method [8] and its derivatives [9]–[11] are designed for deterministic SoS channel simulators, which have the advantage of simulation efficiency. However, these channel simulators still retain some undesirable properties. For example, the cross-correlation function (CCF) of any pair of underlying complex processes is generally not zero for the models in [8]–[10]. The inphase and quadrature components of each underlying complex process have different autocorrelation functions (ACFs) for the model in [11]. To remedy the drawbacks of the deterministic channel simulators in [8]–[11], Zheng and Xiao [12], [13] reintroduced random parameters into the employed sinusoids, resulting in non-ergodic stochastic SoS channel simulators. By averaging over a large number of simulation trials, the developed stochastic channel simulators in [12], [13] can approximate closely the desired statistical properties. However, relatively high computational complexity has to be paid for the channel simulators in [12], [13] due to their non-ergodic stochastic nature.

The method of exact Doppler spread (MEDS) was presented in [14] to determine the parameters of deterministic SoS channel simulators. In [15], the MEDS was revisited and the additional boundary conditions were investigated for producing multiple uncorrelated Rayleigh fading waveforms with the deterministic SoS channel modeling approach. However, with the original MEDS, large values have to be chosen for the numbers of sinusoids when more than 4 uncorrelated Rayleigh processes are produced [15]. This will greatly increase the complexity and therefore, restrict the use of the MIMO channel simulator. An extended version of the MEDS was further presented in [16], which is in nature a quasi-stochastic method but shows better performance than the methods in [12], [13]. In this paper, a new deterministic parameter computation method is proposed for producing multiple uncorrelated Rayleigh fading waveforms without using large numbers of sinusoids for SoS channel simulators. The numerical and simulation results highlight the advantages of the presented channel simulator over other forms of channel simulators in [8]–[16] in both accurate reproduction of all the desired statistical properties of the reference model and efficient implementation due to the retained deterministic nature.

0-7803-9584-0/06/$20.00©2006 IEEE.

The rest of the paper is organized as follows. Section II briefly reviews the desired statistical properties of the reference model. An efficient parameter computation method for deterministic SoS channel simulators is proposed in Section III. Section IV compares the statistical properties of the reference model and the simulation model. Finally, the conclusions are drawn in Section V.

II. The Reference Model

Our purpose is to generate $\mathcal{L}$ uncorrelated Rayleigh fading processes. It is well-known that a Rayleigh process is formed by taking the absolute value of a zero-mean complex Gaussian random process. Ideally, these $\mathcal{L}$ uncorrelated complex Gaussian random processes should satisfy the following criteria: 1) The inphase and quadrature components of each complex process are zero-mean independent real Gaussian random processes with identical ACFs; 2) The CCF of any pair of complex Gaussian random processes must be zero.

Let us denote the desired ℓth ($\ell = 1, 2, \ldots, \mathcal{L}$) Rayleigh fading process by $\zeta_\ell(t)$, which is given by

$$\zeta_\ell(t) = |\mu_\ell(t)| = |\mu_{1,\ell}(t) + j\mu_{2,\ell}(t)| \; . \tag{1}$$

Here, $j = \sqrt{-1}$, $\mu_\ell(t)$ is a zero-mean complex Gaussian random process, $\mu_{1,\ell}(t)$ and $\mu_{2,\ell}(t)$ are uncorrelated real Gaussian random processes with common variance σ_0^2. The envelope PDF of $\zeta_\ell(t)$ is the Rayleigh distribution [8]

$$p_{\zeta_\ell}(x) \;=\; \frac{x}{\sigma_0^2} \exp(-\frac{x^2}{2\sigma_0^2}) \; , \quad x \geq 0 \; . \tag{2}$$

Adopting Clark's two-dimensional isotropic scattering theory [5], the statistical properties of the reference model are specified by the following ACFs and CCFs [17]:

$$\begin{aligned}
r_{\mu_{i,\ell}\mu_{i,\ell}}(\tau) &= E\{\mu_{i,\ell}(t)\mu_{i,\ell}(t+\tau)\} \\
&= \sigma_0^2 J_0(2\pi f_m \tau) && (3)\\
r_{\mu_{1,\ell}\mu_{2,\ell}}(\tau) &= E\{\mu_{1,\ell}(t)\mu_{2,\ell}(t+\tau)\} = 0 && (4)\\
r_{\mu_{2,\ell}\mu_{1,\ell}}(\tau) &= E\{\mu_{2,\ell}(t)\mu_{1,\ell}(t+\tau)\} = 0 && (5)\\
r_{\mu_\ell\mu_\ell}(\tau) &= E\{\mu_\ell^*(t)\mu_\ell(t+\tau)\} \\
&= 2\sigma_0^2 J_0(2\pi f_m \tau) && (6)\\
r_{\mu_\ell\mu_\lambda}(\tau) &= E\{\mu_\ell^*(t)\mu_\lambda(t+\tau)\} = 0 && (7)
\end{aligned}$$

for $i = 1, 2$ and $\ell, \lambda = 1, 2, \ldots, \mathcal{L}$ with $\ell \neq \lambda$. Here, $E\{\cdot\}$ refers to the statistical average operator, f_m is the maximum Doppler frequency, and $J_0(\cdot)$ denotes the zeroth-order Bessel function of the first kind. The goal of our channel simulator is then to reproduce the above desired statistical properties as accurately and efficiently as possible.

III. The Deterministic SoS Channel Simulator

The central limit theorem justifies that a Gaussian random process can be approximated by the superposition of a large number of properly weighted sinusoids. This fact actually serves as the foundation of SoS channel simulators. For our simulation model, the ℓth ($\ell = 1, 2, \ldots, \mathcal{L}$) Rayleigh fading process is modeled as

$$\tilde{\zeta}_\ell(t) = |\tilde{\mu}_\ell(t)| = |\tilde{\mu}_{1,\ell}(t) + j\tilde{\mu}_{2,\ell}(t)| \tag{8}$$

where

$$\tilde{\mu}_{i,\ell}(t) = \sum_{n=1}^{N_i} c_{i,n,\ell} \cos(2\pi f_{i,n,\ell} t + \theta_{i,n,\ell}) \; , \quad i = 1, 2 \; . \tag{9}$$

Here, N_i defines the number of sinusoids, mainly determining the realization expenditure and the accuracy of the resulting channel simulator. The gains $c_{i,n,\ell}$, the discrete frequencies $f_{i,n,\ell}$, and the phases $\theta_{i,n,\ell}$ are real-valued parameters, which are kept constant during simulation. Consequently, $\tilde{\mu}_{i,\ell}(t)$ is a deterministic function and the resulting channel simulator is of deterministic feature. It follows that the statistical properties of our deterministic SoS channel simulator must be calculated by using time averages instead of statistical averages. The envelope PDF $\tilde{p}_{\zeta_\ell}(x)$ of $\tilde{\zeta}_\ell(t)$ can be computed by [14]

$$\tilde{p}_{\zeta_\ell}(x) = x \int_0^{2\pi} \tilde{p}_{\mu_{1,\ell}}(x\cos\theta) \cdot \tilde{p}_{\mu_{2,\ell}}(x\sin\theta) \; d\theta \tag{10}$$

where

$$\begin{aligned}
\tilde{p}_{\mu_{i,\ell}}(x) \;=\; & 2\int_0^\infty \left[\prod_{n=1}^{N_i} J_0(2\pi c_{i,n,\ell}\nu)\right] \cos(2\pi\nu x) \; d\nu, \\
& i = 1, 2 \; . && (11)
\end{aligned}$$

The time-averaged correlation functions of the simulation model, corresponding to (3)–(7) of the reference model, can be expressed as follows:

$$\begin{aligned}
\tilde{r}_{\mu_{i,\ell}\mu_{i,\ell}}(\tau) &= \sum_{n=1}^{N_i} \frac{c_{i,n,\ell}^2}{2} \cos(2\pi f_{i,n,\ell}\,\tau) && (12)\\
\tilde{r}_{\mu_{1,\ell}\mu_{2,\ell}}(\tau) &= 0 \; , \;\; \text{if} \;\; f_{1,n,\ell} \neq \pm f_{2,m,\ell} && (13)\\
\tilde{r}_{\mu_{2,\ell}\mu_{1,\ell}}(\tau) &= \tilde{r}_{\mu_{1,\ell}\mu_{2,\ell}}(-\tau) && (14)\\
\tilde{r}_{\mu_\ell\mu_\ell}(\tau) &= \sum_{i=1}^{2} \tilde{r}_{\mu_{i,\ell}\mu_{i,\ell}}(\tau) + \\
&\quad j\,[\tilde{r}_{\mu_{1,\ell}\mu_{2,\ell}}(\tau) - \tilde{r}_{\mu_{2,\ell}\mu_{1,\ell}}(\tau)] && (15)\\
\tilde{r}_{\mu_\ell\mu_\lambda}(\tau) &= \tilde{r}_{\mu_{1,\ell}\mu_{1,\lambda}}(\tau) + \tilde{r}_{\mu_{2,\ell}\mu_{2,\lambda}}(\tau) + \\
&\quad j\,[\tilde{r}_{\mu_{1,\ell}\mu_{2,\lambda}}(\tau) - \tilde{r}_{\mu_{2,\ell}\mu_{1,\lambda}}(\tau)] \; . && (16)
\end{aligned}$$

In (16), the CCFs $\tilde{r}_{\mu_{i,\ell}\mu_{k,\lambda}}(\tau)$ between $\tilde{\mu}_{i,\ell}(t)$ and $\tilde{\mu}_{k,\lambda}(t)$ ($i, k = 1, 2$ and $\ell, \lambda = 1, 2, \ldots, \mathcal{L}$ with $\ell \neq \lambda$) are given by

$$\tilde{r}_{\mu_{i,\ell}\mu_{k,\lambda}}(\tau) = 0 \; , \;\; \text{if} \;\; f_{i,n,\ell} \neq \pm f_{k,m,\lambda} \; . \tag{17}$$

From (13), (14), and (17), it is clear that the different processes $\tilde{\mu}_{i,\ell}(t)$ and $\tilde{\mu}_{k,\lambda}(t)$ ($i, k = 1, 2$ and $\ell, \lambda = 1, 2, \ldots, \mathcal{L}$; $i = k$ and $\ell = \lambda$ do not hold at the same time) are uncorrelated if and only if

$$f_{i,n,\ell} \neq \pm f_{k,m,\lambda} \tag{18}$$

holds for all $n = 1, 2, \ldots, N_i$ and $m = 1, 2, \ldots, N_k$. This means that the discrete frequencies for different uncorrelated processes must be disjoint. The inequality (18) further allows us to write $\tilde{r}_{\mu_{1,\ell}\mu_{2,\ell}}(\tau) = r_{\mu_{1,\ell}\mu_{2,\ell}}(\tau) = 0$, $\tilde{r}_{\mu_{2,\ell}\mu_{1,\ell}}(\tau) = r_{\mu_{2,\ell}\mu_{1,\ell}}(\tau) = 0$, and $\tilde{r}_{\mu_\ell\mu_\lambda}(\tau) = r_{\mu_\ell\mu_\lambda}(\tau) = 0$. In the following, a new parameter computation method will be introduced concerning how to fulfill the desired boundary constraint (18).

With our proposed method, the phases $\theta_{i,n,\ell}$ in (9) are simply considered as the outcomes of a random generator uniformly distributed over $(0, 2\pi]$, while $c_{i,n,\ell}$ and $f_{i,n,\ell}$ are given by

$$c_{i,n,\ell} = \sigma_0 \sqrt{\frac{2}{N_i}} \tag{19}$$

$$f_{i,n,\ell} = f_m \sin[\frac{(2n-1)\pi}{4N_i}] + (\ell - 1)\varepsilon \tag{20}$$

respectively, where the quantity ε will be defined subsequently. A close observation indicates that the above parameter computation method will reduce to the original MEDS in [14] if $(\ell - 1)\varepsilon = 0$, i.e., $\ell = 1$ or $\varepsilon = 0$. Therefore, we call the proposed method the modified MEDS (MMEDS), which includes the original MEDS as a special case.

The substitution of (20) into (18) tells us that

$$\frac{N_1}{N_2} \neq \frac{2n-1}{2m-1} \tag{21}$$

for all $n = 1, 2, \ldots, N_1$ and $m = 1, 2, \ldots, N_2$ must be fulfilled in order to guarantee $f_{1,n,\ell} \neq \pm f_{2,m,\ell}$. This implies that that the ratio of N_1 to N_2 should not be the ratio of two odd numbers. In this paper, we choose $N_2 = N_1 + 1$ for simplicity. In order to satisfy the condition $f_{i,n,\ell} \neq \pm f_{k,m,\lambda}$ ($i, k = 1, 2$ and $\ell, \lambda = 1, 2, \ldots, \mathcal{L}$ with $\ell \neq \lambda$), the quantity ε must be chosen in such a way that the following inequality is fulfilled

$$\varepsilon \neq \frac{f_m}{\pm(\lambda - \ell)} \{\sin[\frac{(2n-1)\pi}{4N_i}] \mp \sin[\frac{(2m-1)\pi}{4N_k}]\}. \tag{22}$$

Given any f_m, $\mathcal{L}$, N_1, and N_2, the values of the right side of the above inequality can easily be calculated. Then, the quantity ε can be determined.

A properly selected ε will make the CCF of any pair of generated processes be zero, which is one of the desired properties. In the following, we will investigate the impact of ε on the approximation quality of the ACFs, e.g., $\tilde{r}_{\mu_{i,\ell}\mu_{i,\ell}}(\tau) \approx r_{\mu_{i,\ell}\mu_{i,\ell}}(\tau)$. An appropriate measure of the error between the approximate ACF $\tilde{r}_{\mu_{i,\ell}\mu_{i,\ell}}(\tau)$ in (12) and the exact ACF $r_{\mu_{i,\ell}\mu_{i,\ell}}(\tau)$ in (3) is the following mean-square error (MSE) defined by

$$E_{i,\ell} = \frac{1}{\tau_{max}} \int_0^{\tau_{max}} [r_{\mu_{i,\ell}\mu_{i,\ell}}(\tau) - \tilde{r}_{\mu_{i,\ell}\mu_{i,\ell}}(\tau)]^2 d\tau \tag{23}$$

where τ_{max} denotes an appropriate time interval $[0, \tau_{max}]$ over which the approximation of $r_{\mu_{i,\ell}\mu_{i,\ell}}(\tau)$ is of interest. According to our investigations, the value $\tau_{max} = N_i/(2f_m)$ has turned out to be suitable. Fig. 1 shows the MSE $E_{i,\ell}$ of the ACF as a function of the quantity ε with different values of ℓ. In this example, we used $f_m = 91$ Hz, $\sigma_0^2 = 1$, $\mathcal{L} = 4$, and $N_i = 10$. It can clearly be observed that the MSE increases with the increase of the absolute value of ε, while the minimum MSE is obtained when $\varepsilon = 0$. This suggests us to choose an infinitesimal value for ε, e.g., $\varepsilon = 10^{-7}$, as long as it satisfies (22). Compared between $\mathcal{L} = 4$ different processes, the best approximation to the desired ACF is obtained when $\ell = 1$, while $\ell = 4$ provides the worst fitting. From Fig. 1, we can conclude that the original MEDS ($\varepsilon = 0$ or $\ell = 1$) provides the best fitting result. In Fig. 2, we compare the ACFs of the quadrature component for the reference model, the simulation model by using the MEDS ($\varepsilon = 0$) and the MMEDS with $\varepsilon = 0.01$ and $\varepsilon = 1$. Here, $\sigma_0^2 = 1$, $N_i = 10$, and $\ell = 2$ were used. It is obvious that the best approximation result of the ACF is obtained by using the MEDS. When $\varepsilon = 0.01$, the resulting ACF with the MMEDS is nearly indistinguishable from that obtained by using the MEDS. Even when $\varepsilon = 1$, the approximation quality of the resulting ACF is still acceptable.

IV. Simulation Results and Discussions

In this section, the statistical properties of the resulting deterministic SoS channel simulator by using the MMEDS will be investigated in detail and compared with those of the reference model.

We can easily show that the deterministic process $\tilde{\mu}_{i,\ell}(t)$ in (9) with the parameters determined by the MMEDS has the desired mean value 0 and variance σ_0^2. The conditions (21) and (22) make sure that the inequality (18) is fulfilled, which guarantees that the CCFs shown in (13), (14), and (16) are identical with those in (4), (5), and (7), respectively. It can also be shown that the substitution of (19) into (10) results for $N_i \to \infty$ in $\tilde{p}_{\zeta_\ell}(x) \to p_{\zeta_\ell}(x)$. Similarly, with the help of (19) and (20), $\tilde{r}_{\mu_{i,\ell}\mu_{i,\ell}}(\tau) \to r_{\mu_{i,\ell}\mu_{i,\ell}}(\tau)$ and $\tilde{r}_{\mu_\ell\mu_\ell}(\tau) \to r_{\mu_\ell\mu_\ell}(\tau)$ can be obtained when $N_i \to \infty$ and $\varepsilon \to 0$. In the following, we demonstrate the approximation qualities of $\tilde{p}_{\zeta_\ell}(x) \approx p_{\zeta_\ell}(x)$, $\tilde{r}_{\mu_{i,\ell}\mu_{i,\ell}}(\tau) \approx r_{\mu_{i,\ell}\mu_{i,\ell}}(\tau)$, and $\tilde{r}_{\mu_\ell\mu_\ell}(\tau) \approx r_{\mu_\ell\mu_\ell}(\tau)$ when finite values of N_i are taken. A fixed value 10^{-7} was selected for the quantity ε. Unless specified, $\ell = 2$ was used to get the results.

Fig. 3 shows the excellent agreement between the Rayleigh distribution ($\sigma_0^2 = 1$) and the approximate envelope PDF with $N_1 = 9$ and $N_2 = 10$. The corresponding simulated envelope PDF obtained from the output of the channel simulator is also presented in the figure to validate the analytical result. Fig. 4 illustrates the ACF with $N_i = 10$ and the CCF with $N_1 = 9$ and $N_2 = 10$ by using the MMEDS. Again, the simulation results are provided for reasons of verification. The ACF and CCF of the reference model are also demonstrated in the figure for comparison purposes. Clearly, the CCFs of the reference model and simulation model are equal to 0 for all τ. The ACF of the simulation model matches almost perfectly the desired one if the normalized time delay $f_m\tau$ is within the interval [0, $N_i/2$], which includes N_i zero-crossings of the ACF. In case that $f_m\tau > N_i/2$, the ACFs of the simulation model and reference model will diverge gradually and never converge again. A better approximation over larger time delays can only be achieved with the increase of N_i. It is also shown in Fig. 5 that the ACFs of the complex envelope for the reference model and simulation model are very close to each other when $f_m\tau$ is located in the interval $[0, \min\{N_1, N_2\}/2]$. Due to the fact that short time delays, e.g., $f_m\tau \leq 0.3$ [18], are of more interest for most communication systems, the MMEDS with small numbers of sinusoids N_i is actually an excellent method in

terms of the above interested correlation properties. In Fig. 6, two uncorrelated simulated fading envelops are presented by using the MMEDS with $\sigma_0^2 = 1$, $f_m = 91$ Hz, $N_1 = 9$, $N_2 = 10$, and $\ell = 2, 3$.

Compared with the MEDS, the proposed MMEDS provides the same approximation to the desired PDF but worse approximations to the desired quadrature and complex ACFs when $\ell > 1$. However, the performance degradation can completely be neglected as long as an infinitesimal value is chosen for the quantity ε. On the other hand, the MMEDS does not require the increase of the numbers of sinusoids when more uncorrelated processes are produced, while the MEDS [15] needs. This promising advantage of the MMEDS allows us to simulate a very large number of uncorrelated fading processes without increasing the complexity of the channel simulator.

Compared with the non-ergodic stochastic SoS channel simulators in [12], [13], the presented deterministic SoS channel simulator with the MMEDS has much better simulation efficiency since the calculation of its statistical properties does not need the average of a number of random trials. With the same numbers of sinusoids, our deterministic channel simulator has similar performance to that of the stochastic simulators in [12], [13] in terms of the amplitude PDF. The performance of the deterministic channel simulator is comparable to or even better than that of the stochastic channel simulators in [12], [13] for the approximation of the ACFs inside the specified time delay ranges, e.g., $f_{max}\tau \in [0, N_{i,\ell}/2]$ for $r_{\mu_{i,\ell}\mu_{i,\ell}}(\tau)$. Outside the specified time delay ranges, which may not be relevant for communication systems [18], the stochastic channel simulators in [12], [13] provide much better approximation to the desired ACFs than our deterministic channel simulator. Furthermore, the accuracy of the statistic properties of the non-ergodic stochastic channel simulators can be improved by increasing either the numbers of sinusoids or the number of random trials to be averaged. On the other hand, the performance of the presented deterministic channel simulator can only be improved by increasing the numbers of sinusoids.

It is well known that multiple cross-correlated processes can be obtained by using a linear combination of uncorrelated processes [17], [19]. As shown in [19], the above presented deterministic channel simulator can easily be extended to the generation of multiple cross-correlated Rayleigh fading processes for simulating more realistic MIMO channels.

V. Conclusion

In this paper, a new parameter computation method, the so-called MMEDS, for deterministic SoS channel simulators is presented to generate multiple uncorrelated Rayleigh fading processes, which are useful for the modeling of MIMO, wideband, and diversity-combined multipath fading channels. Compared with the MEDS, the MMEDS provides similar good approximations to the desired statistical properties of the reference model, while requires much lower numerical computation expenditure. In order to guarantee the uncorrelatedness between different simulated fading processes, the MMEDS is quite simple and straightforward. The MEDS, however, demands the increase of the numbers of sinusoids and therefore the increase of the channel simulator complexity. Clearly, the MMEDS overall outperforms the MEDS and is highly recommended for the simulation of a large number of uncorrelated fading processes.

References

[1] 3GPP TR 25.913, "Requirements for evolved Universal Terrestrial Radio Access (UTRA) and Universal Terrestrial Radio Access Network (UTRAN)," (RP-050150, REV-05013), 2005.

[2] 3GPP, TR 25.996, "Spatial channel model for Multiple Input Multiple Output (MIMO) simulations (Rel. 6)," 2003.

[3] 3GPP, R1-050586, "Wideband SCM," 2005.

[4] 3GPP, R1-050680, "Simulation assumptions and evaluation for EUTRA," 2005.

[5] R. H. Clarke, "A statistical theory of mobile-radio reception," *Bell Syst. Tech. J.*, vol. 47, pp. 957–1000, July/Aug. 1968.

[6] S.O. Rice, "Mathematical analysis of random noise," *Bell Syst. Tech. J.*, vol. 23, pp. 282–332, July 1944.

[7] S.O. Rice, "Mathematical analysis of random noise," *Bell Syst. Tech. J.*, vol. 24, pp. 46–156, Jan. 1945.

[8] W. C. Jakes, Ed., *Microwave Mobile Communications*. New Jersey: IEEE Press, 1994.

[9] P. Dent, G. E. Bottomley, and T. Croft, "Jakes fading model revisited," *Electron. Lett.*, vol. 29, no. 13, pp. 1162–1163, June 1993.

[10] Y. B. Li and Y. L. Guan, "Modified Jakes model for simulating multiple uncorrelated fading waveforms," *Proc. IEEE ICC '00*, New Orleans, LA, USA, June 2000, pp. 46–49.

[11] Y. X. Li and X. J. Huang, "The simulation of independent Rayleigh faders," *IEEE Trans. Commun.*, vol. 50, no. 9, pp. 1503–1514, Sept. 2002.

[12] Y. R. Zheng and C. S. Xiao, "Improved models for the generation of multiple uncorrelated Rayleigh fading waveforms," *IEEE Commun. Lett.*, vol. 6, no. 6, pp. 256–258, June 2002.

[13] Y. R. Zheng and C. S. Xiao, "Simulation models with correct statistical properties for Rayleigh fading channels," *IEEE Trans. Commun.*, vol. 51, no. 6, pp. 920–928, June 2003.

[14] M. Pätzold, *Mobile Fading Channels*. Chichester: John Wiley & Sons, 2002.

[15] C. X. Wang and M. Pätzold, "Methods of generating multiple uncorrelated Rayleigh fading processs," *Proc. IEEE VTC '03-Spring*, Jeju, Korea, April 2003, pp. 510–514.

[16] M. Pätzold, B. O. Hogstad, D. Kim, and S. Kim, "A new design concept for high-performance fading channel simulators using set partitioning," *Proc. IEEE WPMC '05*, Aalborg, Denmark, Sept. 2005.

[17] G. L. Stüber, *Principles of Mobile Communications*. Boston: Kluwer Academic Publishers, 2nd edition, 2001.

[18] P. Hoeher and A. Steingass, "Modeling and emulation of multipath fading channels using controlled randomness," *Proc. ITG-Fachtagung "Wellenausbreitung bei Funksystemen und Mikrowellensystemen"*, Oberpfaffenhofen, Germany, May 1998, pp. 209–220.

[19] C. X. Wang and M. Pätzold, "Efficient simulation of multiple cross-correlated Rayleigh fading channels," *Proc. IEEE PIMRC '03*, Beijing, China, Sept. 2003, pp. 1526–1530.

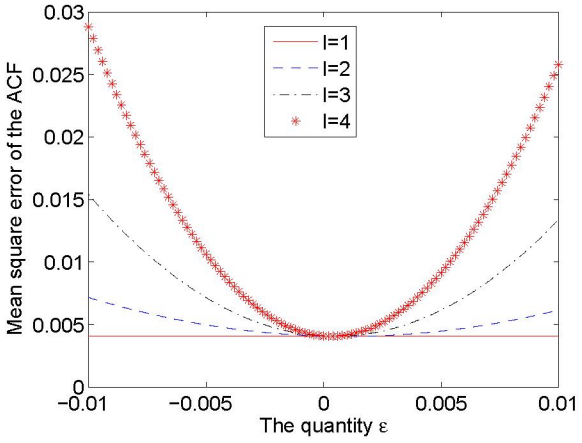

Fig. 1. The mean square error of the ACF by using the MMEDS ($\sigma^2{}_0 = 1$, $f_m = 91$ Hz, $N_i = 10$, and $\mathcal{L} = 4$).

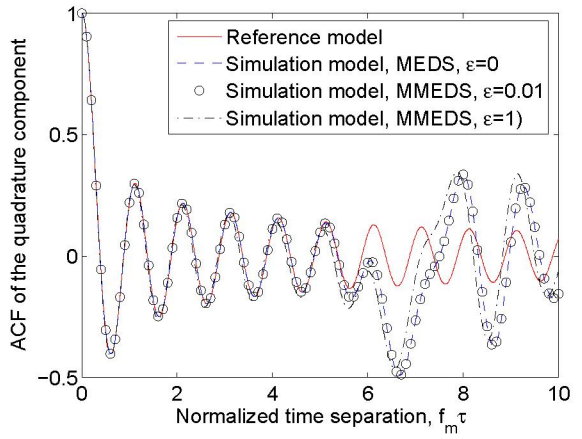

Fig. 2. The ACFs of the quadrature component for the reference model and the simulation model by using the MEDS and the MMEDS ($\sigma^2{}_0 = 1$, $N_i = 10$, and $\ell = 2$).

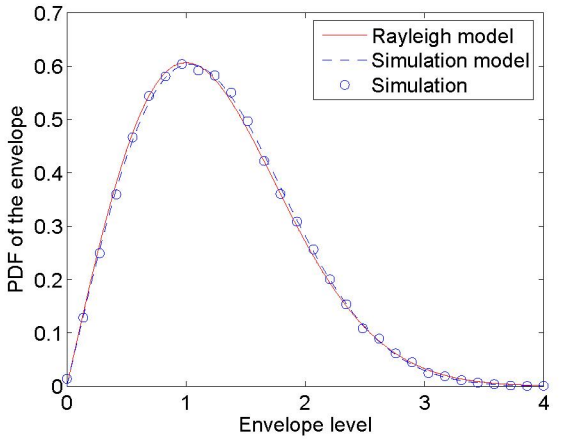

Fig. 3. The envelope PDFs of the Rayleigh model and the simulation model by using the MMEDS ($\sigma^2{}_0 = 1$, $N_1 = 9$, and $N_2 = 10$).

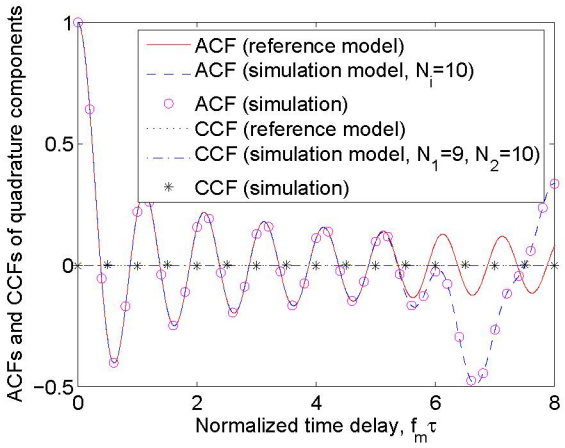

Fig. 4. The ACFs and CCFs of the quadrature components for the reference model and the simulation model by using the MMEDS ($\sigma^2{}_0 = 1$ and $\ell = 2$).

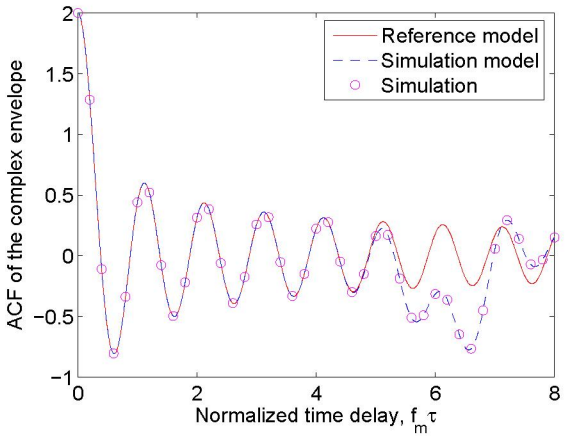

Fig. 5. The ACFs of the complex envelope for the reference model and the simulation model by using the MMEDS ($\sigma^2{}_0 = 1$, $\ell = 2$, $N_1 = 9$, and $N_2 = 10$).

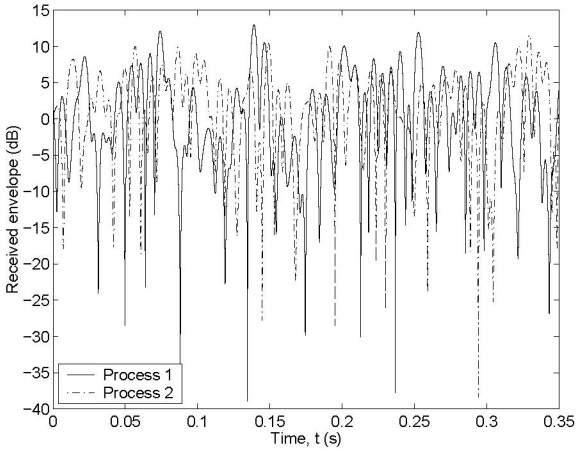

Fig. 6. Uncorrelated simulated fading envelopes by using the MMEDS ($\sigma^2{}_0 = 1$, $f_m = 91$ Hz, $N_1 = 9$, $N_2 = 10$, and $\ell = 2, 3$).